Physical modeling and performance bounds for device-free localization systems

V. Rampa(*), S. Savazzi(*), M. Nicoli(+), M. D'Amico(+)
Consiglio Nazionale delle Ricerche (CNR) - IEIIT (*), Politecnico di Milano - DEIB (+)

Device-free passive (non-cooperative) localization systems

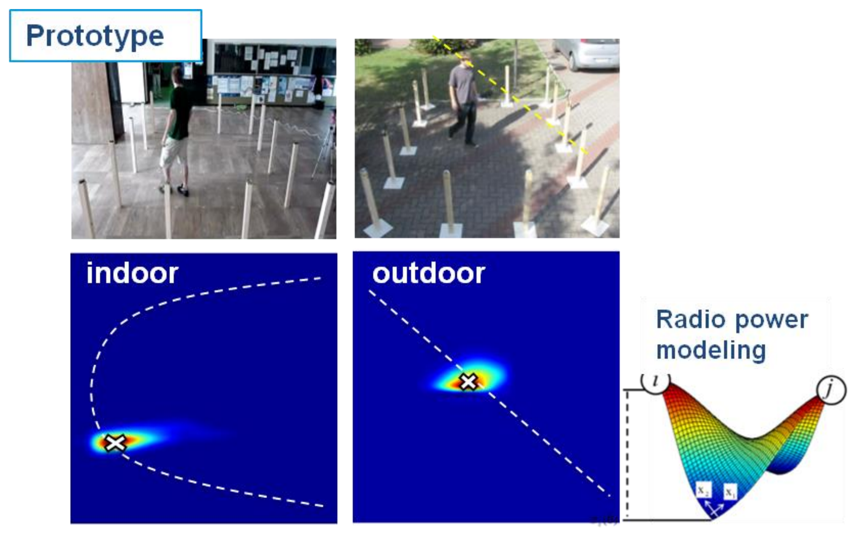

- **DFL network:** allows to locate and track passive objects moving in an area monitored by dense network of low-power wireless sensors [1]-[2] (i.e., targets not carrying electronic devices)

- **How it works**
  - Wireless nodes cooperatively exchange radio signals and measure the received signal strength (RSS).
  - The object (target) causes fluctuations of the signal strength field that depends on the position of the target thus allowing to localize the object.

Active Localization

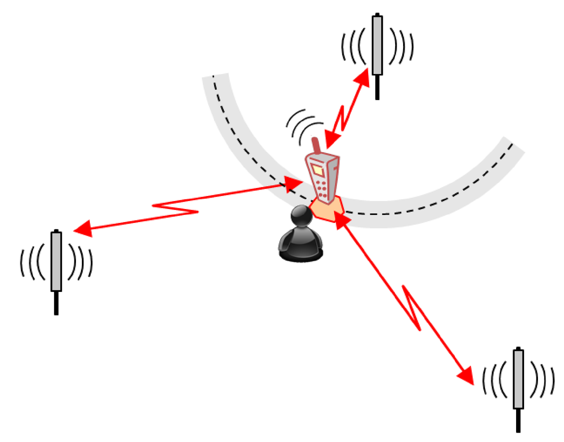

Passive Localization (DFL)

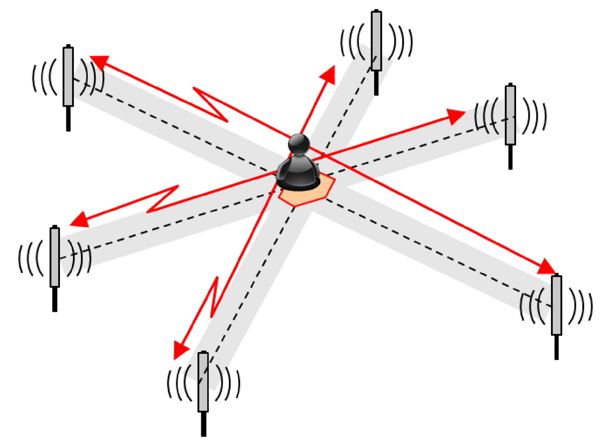

- **Active Localization:** the target being tracked is equipped with a radio device sending probe signals.

- **Passive Localization (DFL):** the target being tracked does not need to carry any electronic device

Contributions

- A novel and analytically tractable model for prediction of the body-induced propagation loss is developed. The model is suitable for DFL applications [3]: the dominant static component and the stochastic fluctuations of the power loss are derived as a function of the target location.

- The model, that extends the validity of the one employed in [4],[5] for objects placed only along the line-of-sight (LOS) path, is exploited to analytically compute the Cramer-Rao Lower Bound (CRLB) to evaluate the theoretical limits to localization accuracy over a 2D link area.

[1] M. Youssef, M. Mah, and A. Agrawala, "Challenges: Device-free passive localization for wireless environments," in Proceedings of the 13th Annual ACM International Conference on Mobile Computing and Networking (MobiCom '07). ACM, 2007, pp. 222–229.
[2] N. Patwari and J. Wilson, "RF Sensor Networks for Device-Free Localization: Measurements, Models, and Algorithms," Proceedings of the IEEE, vol. 98, no. 11, pp. 1961–1973, Nov 2010.
[3] S. Savazzi, S. Sigg, M. Nicoli, et al., "Device-Free Radio Vision for Assisted Living: Leveraging wireless channel quality information for human sensing," IEEE Signal Processing Magazine, vol. 33, no. 2, pp. 45-58, March 2016.
[4] S. Savazzi, M. Nicoli, et al., "A Bayesian approach to Device-Free Localization: Modeling and experimental assessment," IEEE Journal of Selected Topics in Signal Processing, vol. 8, no. 1, pp. 16–29, Feb 2014.
[5] S. Obayashi and J. Zander, "A body-shadowing model for indoor radio communication environments," IEEE Transactions on Antennas and Propagation, vol. 46, no. 6, pp. 920–927, Jun 1998.

Physical modeling of human induced shadowing

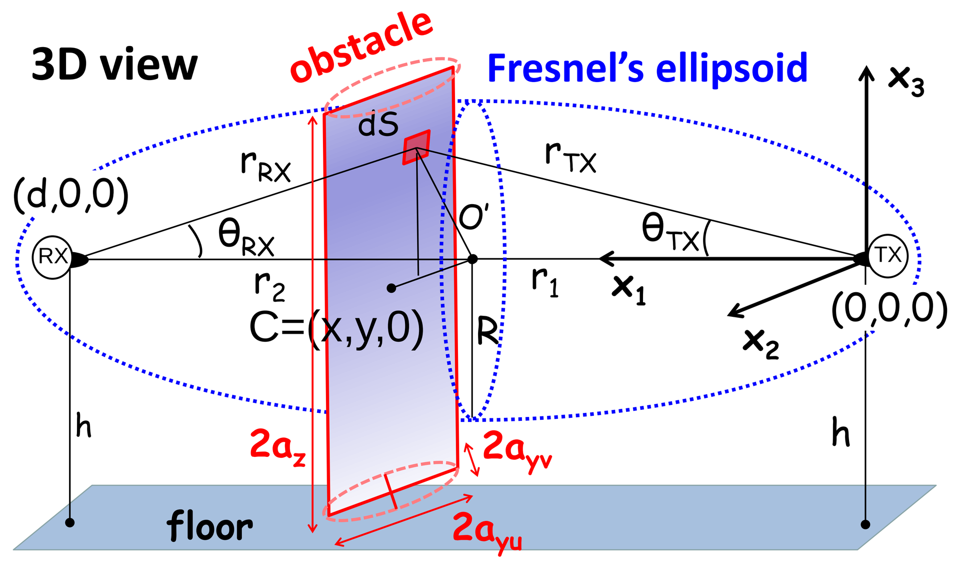

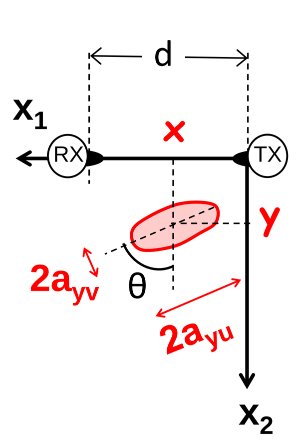

Electric field. The electric field at the RX can be predicted as generated by a virtual array of Huygens' sources located on the obstacle plane and not belonging to the obstacle itself.
The electric field ratio

$$|E/E_0|^2 = \mathrm{G}\left(\mathbf{X}|\,a_y, a_z\right)$$

can be derived in closed form and approximated as

$$\mathrm{G}(\mathbf{X}|a_y) \simeq \left[\frac{R}{\pi a_y}\cos\left(2\pi f_y y\right)\right]^2,\ \forall \mathbf{X} \in \mathcal{H}_{\mathrm{W},d}$$

This approximation captures the physical effects of an obstructing target located inside the link sensitivity $\mathcal{H}_{\mathrm{W},d}$ where the target influences the RF field:

$$\mathcal{H}_{\mathrm{W},d} \triangleq \left\{\mathbf{X} \in \mathcal{H}_{\mathrm{W},d} : 0 \le x \le d,\ |y| \le \tfrac{1}{2}\mathrm{W}(x)\right\}$$

with

$$\mathrm{W}(x) = 1/f_y = \lambda x\,(d-x)\,/a_y d.$$

This area is an eye-shaped zone centered on the LOS, with length *d* and width W(*x*) varying with *x*.

RSS modeling. Goal is to introduce a tractable mathematical model that relates RSS *P* to the location **X** and used for the localization of the target.

Log-normal modeling

$$P = \begin{cases} \mathcal{P}_0 = h_0 + w_0, & \mathbf{X} \notin \mathcal{H}_{\mathrm{W},d} \\ \mathcal{P}_1 = h_1(\mathbf{X},\theta) + w_1, & \mathbf{X} \in \mathcal{H}_{\mathrm{W},d} \end{cases}$$

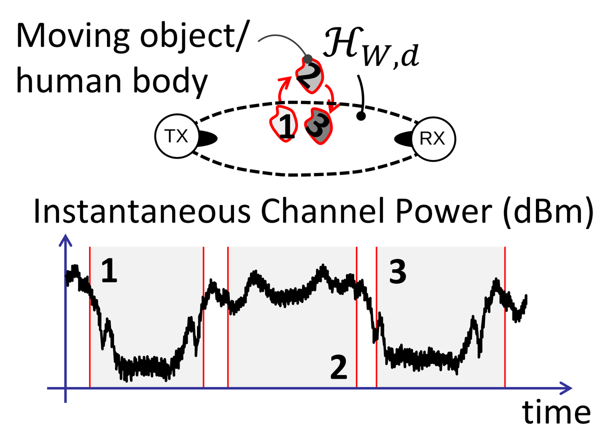

The target-induced perturbations are evaluated in terms of the average path-loss and power fluctuations assuming that the target is standing in **X** with varying orientation θ. The target presence modifies both the RSS mean and the variance

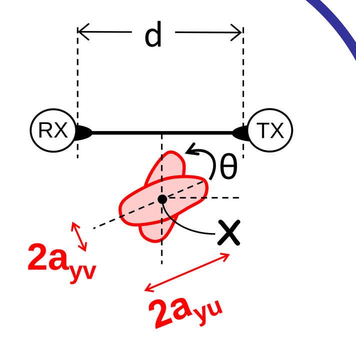

with $\mu_1(\mathbf{X}) = \mathrm{E}_{\theta,\mathrm{w}_1}[\mathcal{P}_1]$ $\quad \sigma_1^2(\mathbf{X}) = \mathrm{Var}_{\theta,\mathrm{w}_1}[\mathcal{P}_1]$

Multipath reflections → Diffraction effects

$$\mu_1(\mathbf{X}) = h_0 + \underbrace{\Delta h_C + \mathrm{E}_\theta\left[\mathrm{G}\left(\mathbf{X}|a_y(\theta),a_z\right)|_{\mathrm{dB}}\right]}_{\Delta\mu(\mathbf{X})}$$

$$\sigma_1^2(\mathbf{X}) = \sigma_0^2 + \underbrace{\Delta\sigma_C^2 + \mathrm{Var}_\theta\left[\mathrm{G}\left(\mathbf{X}|a_y(\theta),a_z\right)|_{\mathrm{dB}}\right]}_{\Delta\sigma^2(\mathbf{X})}$$

$$\Delta\mu(\mathbf{X}) = \Delta h_C + 5\log_{10}\left[\mathrm{G}_u(\mathbf{X})\cdot\mathrm{G}_v(\mathbf{X})\right]$$

$$\Delta\sigma^2(\mathbf{X}) = \Delta\sigma_C^2 + \left(5\log_{10}\left[\frac{\mathrm{G}_u(\mathbf{X})}{\mathrm{G}_v(\mathbf{X})}\right]\right)^2$$

$$\mathrm{G}_v(\mathbf{X}) = \mathrm{G}(\mathbf{X}|a_y,a_z)\,|_{a_y=a_{yv}}$$

$$\mathrm{G}_u(\mathbf{X}) = \mathrm{G}(\mathbf{X}|a_y,a_z)\,|_{a_y=a_{yu}}$$

Diffraction terms evaluated analytically. Multipath terms from calibration

Experimental model validation

- RSS data acquired with and w/o the target by pre-calibrated SDR devices (USRP N210) (2 dBi vertical monopole antennas)
- RF transceiver: single unmodulated carrier waveform at frequency 2.486 GHz.
- Comparative EM simulations obtained with software tool FEKO (2D PEC obstacle with and w/o floor: $a_{yu} = 0.275$ m, $a_{yv} = 0.12$ m)
- Main model parameters: $\Delta\sigma_C^2 = 1$ dB, $\Delta h_C = 0$ dB, $h = 0.9$ m, $d = 5$ m

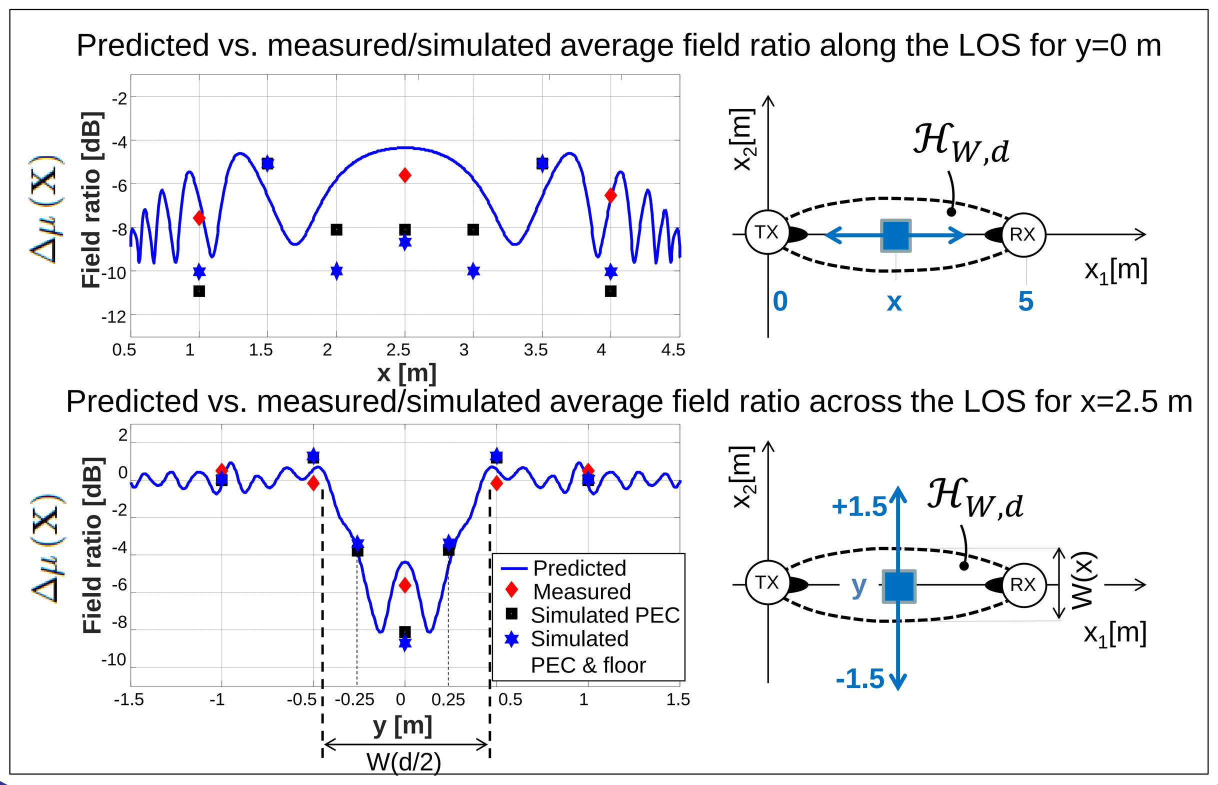

Localization accuracy bounds (CRLB)

The maximum DFL positioning accuracy evaluated using the CRLB approach.

- L power measurements (links) being independent, with joint log-likelihood function, $\ln\mathcal{L}(\mathbf{X}) = \sum_{\ell=1}^{L}\ln\mathcal{L}_\ell(\mathbf{X})$.
- CRLB matrix **C(X)** provides a lower bound to the covariance for any unbiased estimator $\hat{\mathbf{X}}$ of the target position $\mathrm{E}[(\hat{\mathbf{X}}-\mathbf{X})(\hat{\mathbf{X}}-\mathbf{X})^{\mathrm{T}}] \ge \mathbf{C}(\mathbf{X}) = \mathbf{F}^{-1}(\mathbf{X})$
- Fisher Information Matrix **F** with:

$$F_{i,j} = \mathrm{E}\left[\left(\sum_{\ell=1}^{L}\frac{\partial\ln\mathcal{L}_\ell(\mathbf{X})}{\partial x_i}\right)\left(\sum_{\ell=1}^{L}\frac{\partial\ln\mathcal{L}_\ell(\mathbf{X})}{\partial x_j}\right)\right]$$

- FIM derived analytically using the proposed model:

$$F_{i,i} = \sum_{\ell=1}^{L}\frac{1}{\sigma_{1,\ell}^2(\mathbf{X})}\left[\left(\frac{\partial\mu_{1,\ell}(\mathbf{X})}{\partial x_i}\right)^2 + 2\left(\frac{\partial\sigma_{1,\ell}(\mathbf{X})}{\partial x_i}\right)^2\right]$$

$$F_{i,j} = \sum_{\ell=1}^{L}\frac{\frac{\partial\mu_{1,\ell}(\mathbf{X})}{\partial x_i}\frac{\partial\mu_{1,\ell}(\mathbf{X})}{\partial x_j} + 2\frac{\partial\sigma_{1,\ell}(\mathbf{X})}{\partial x_i}\frac{\partial\sigma_{1,\ell}(\mathbf{X})}{\partial x_j}}{\sigma_{1,\ell}^2(\mathbf{X})}.$$

Single link CRLB (bottom figure) with highlighted obstacle size and sensitivity area

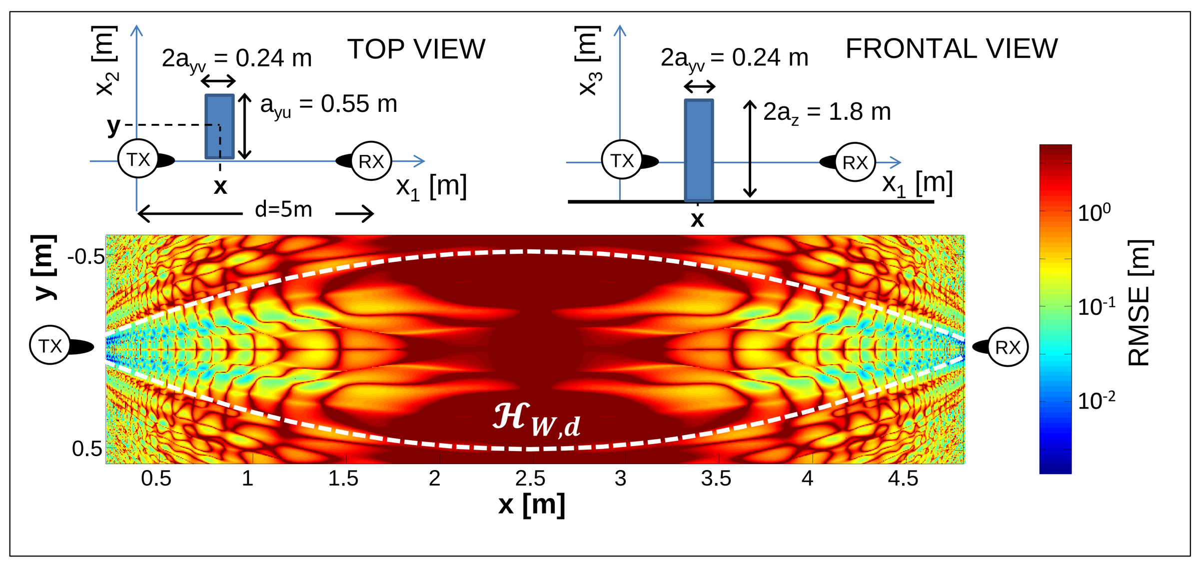

CRLB for the 4-node (L=2) topology (figure on the right). Accuracy is highly space-varying: the model predicts a higher sensing capability of the radio link near the TX and RX, w.r.t sensitivity for targets located in-between. Reduced sensitivity counter-balanced by improving the multiplicity of the links.